Twenty-three cycles of changing open solar magnetic flux

Article

Twenty-three cycles of changing open solar magnetic flux

M. Lockwood[1]
Rutherford Appleton Laboratory, Chilton, Didcot, Oxfordshire, UK

Received 4 April 2002; revised 12 June 2002; accepted 18 June 2002; published 21 March 2003.

[1] This paper presents a comparison of various estimates of the open solar flux, deduced from measurements of the interplanetary magnetic field, from the aa geomagnetic index and from photospheric magnetic field observations. The first two of these estimates are made using the Ulysses discovery that the radial heliospheric field is approximately independent of heliographic latitude, the third makes use of the potential-field source surface method to map the total flux through the photosphere to the open flux at the top of the corona. The uncertainties associated with using the Ulysses result are 5%, but the effects of the assumptions of the potential field source surface method are harder to evaluate. Nevertheless, the three methods give similar results for the last three solar cycles when the data sets overlap. In 11-year running means, all three methods reveal that 1987 marked a significant peak in the long-term variation of the open solar flux. This peak is close to the solar minimum between sunspot cycles 21 and 22, and consequently the mean open flux (averaged from minimum to minimum) is similar for these two cycles. However, this similarity between cycles 21 and 22 in no way implies that the open flux is constant. The long-term variation shows that these cycles are fundamentally different in that the average open flux was rising during cycle 21 (from consistently lower values in cycle 20 and toward the peak in 1987) but was falling during cycle 22 (toward consistently lower values in cycle 23). The estimates from the geomagnetic aa index are unique as they extend from 1842 onwards (using the Helsinki extension). This variation gives strong anticorrelations, with very high statistical significance levels, with cosmic ray fluxes and with the abundances of the cosmogenic isotopes that they produce. Thus observations of photospheric magnetic fields, of cosmic ray fluxes, and of cosmogenic isotope abundances all support the long-term drifts in open solar flux reported by *Lockwood et al.* [1999a, 1999b]. *INDEX TERMS:* 7524 Solar Physics, Astrophysics, and Astronomy: Magnetic fields; 2104 Interplanetary Physics: Cosmic rays; 2134 Interplanetary Physics: Interplanetary magnetic fields; 7536 Solar Physics, Astrophysics, and Astronomy: Solar activity cycle (2162); 1650 Global Change: Solar variability; *KEYWORDS:* solar magnetic fields, heliosphere, cosmic rays

Citation: Lockwood, M., Twenty-three cycles of changing open solar magnetic flux, *J. Geophys. Res.*, *108*(A3), 1128, doi:10.1029/2002JA009431, 2003.

1. Introduction

[2] The open magnetic flux of the Sun has been estimated using two different and entirely independent procedures. The first uses solar surface magnetograms which give the line-of-sight component of the photospheric magnetic field. This is mapped up to a hypothetical surface called the "coronal source surface" where the field is purely radial. In order to do this, it is assumed that there are no currents in the corona between the photosphere and the source surface so that $\nabla \times \mathbf{B} = 0$. The field is assumed to be radial in the photosphere to convert the observed line-of-sight components to the field perpendicular to the surface; thus information has never been available from the poles. The source surface is usually assumed to be spherical at a heliocentric distance of $r = 2.5\ R_s$ (where a mean solar radius, $1\ R_s = 6.96 \times 10^8$ m). The solution to Laplace's equation yields the coronal field lines, and those that reach from the photosphere to coronal source surface are classed as open and the total flux they constitute determined. Although it is a very useful idealised concept, there is no a priori reason why the source surface should be spherical and heliocentric; indeed it may not exist at all. These "potential field source surface" (PFSS) methods [*Schatten*, 1999; *Wang and Sheeley*, 1995] therefore give an estimate of the open flux, but there are uncertainties arising from the several assumptions made and there is no direct way to quantify these.

[3] There are concerns about using the PFSS method on the National Solar Observatory (NSO) Kitt Peak photospheric data (taken in the 868.8 nm Fe I line) because they have an uncertain zero level. Data from the Mount Wilson Observatory (MWO) and the Wilcox Solar Observatory

[1]Also at Department of Physics and Astronomy, Southampton University, Southampton, UK.

0148-0227/03/2002JA009431$09.00

(WSO) can be used but a latitude-dependent "Ulrich correction" must be employed [*Wang and Sheeley*, 1995, 2002]. This is because at both MWO and WSO the magnetograph observations are made using the Fe I line at 525 nm and the photospheric field is concentrated into small unresolved flux tubes of field strength of the order of 0.1 T which causes a Zeeman splitting that is comparable to the line width. This means that the magnetograph intensity is saturated and the magnetic field is underestimated. This effect is less severe near the limb where higher altitudes of the photosphere are observed and field strengths are lower. Therefore along the central meridian the correction needed for this line saturation is latitude dependent. The correction function has been computed by *Ulrich* [1992] by comparisons with the 523.3 nm line which saturates at a higher field. The data used here are from WSO for 1976–1995 and the MWO data are used only for the data gaps of 1971–1976 and 1995–2000.

[4] The second, more direct, method for computing open flux has been made possible by the discovery by the Ulysses spacecraft that the radial component of the heliospheric field is independent of heliographic latitude [*Balogh et al.*, 1995; *Lockwood et al.*, 1999b; *Smith et al.*, 2001]. This means that there are sheet currents but no volume currents in the heliosphere. This discovery has been explained in terms of the low plasma β of the expanding solar wind at about 1.5 $R_s < r < 10\ R_s$, where nonradial flow allows the magnetic flux to redistribute itself to give latitude independent tangential magnetic pressure and thus a uniform radial field component [*Suess and Smith*, 1996; *Suess et al.*, 1996].

[5] Because of this result, the radial field seen near Earth B_{r1} can be used to compute the total (signed) flux threading a heliocentric sphere of radius $R_1 = 1$ AU (1AU is the mean Earth-Sun distance, 150×10^6 km):

$$F'_S = 4\pi R_1^2 |B_{r1}|/2 \quad (1)$$

The factor 2 arises because half the flux through this surface is outward and half is inward. Section 2.1 analyzes the errors introduced by the use of equation (1). Here and in section 2.1 we use the prime to denote that the open flux is estimated from near-Earth measurements assuming the Ulysses result that the radial field is independent of latitude.

[6] The near-Earth and PFSS methods can yield consistent results but only if the latitude-dependent saturation correction is applied to the photospheric data before the PFSS method is applied. *Wang and Sheeley* [1995] were able to match to the radial field seen at Earth during solar cycles 20 and 21, again using the assumption that the radial field B_r is independent of latitude in the heliosphere. Note that this procedure assumes that there are no currents in the corona between the photosphere and the coronal source surface and that there are sheet currents, but no volume current, in the heliosphere between the source surface and the Earth's orbit. Recent work by *Wang and Sheeley* [2002] shows that the near-Earth and the PFSS methods have remained in good general agreement for the more recent data from cycles 22 and 23.

[7] There is one additional difference between the near-Earth and the PFSS methods. The PFSS method quantifies the open flux threading the hypothetical coronal source surface (usually assumed to be at $r = 2.5\ R_s$). On the other hand, the near-Earth method quantifies the flux threading a fixed heliocentric sphere at $r = R_1$. From flux transport over interplanetary magnetic field (IMF) monitors during the solar wind transit times from $r = 2.5\ R_s$ to $r = R_1$, *Lockwood* [2002b] has quantified the open flux F_o which, at any one time, threads the assumed coronal source surface ($r = 2.5\ R_s$) but which closes in the inner heliosphere, such that it does not thread the spherical surface at $r = R_1$. The results for hourly data show symmetric distributions of F_o about zero, with upper and lower deciles of $\pm 0.2\ F'_S$. The uncertainty associated with such flux averages to very small values on longer timescales ($\pm 0.02\ F'_S$ in annual means).

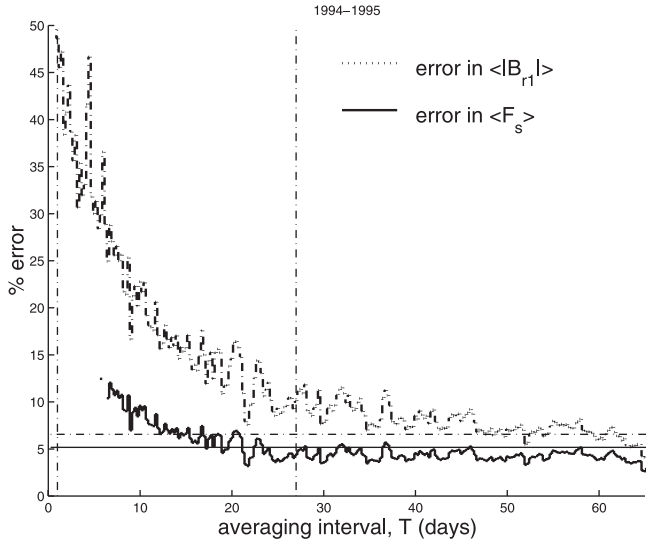

Figure 1. Analysis of errors for the first perihelion pass of Ulysses. The dotted line gives the percent deviation of the radial field seen at Earth and at Ulysses (range corrected and lagged by the propagation time from R_1 to r_U), 100 $[(r_U/R_1)^2|B_{rU}| - |B_{r1}|]/|B_{r1}|$. The solid line is the consequent error in using equation (1) to quantify the open solar flux (from *Lockwood et al.* [2003]).

[8] Recently, *Arge et al.* [2002] have noted that the open flux deduced from the PFSS method is broadly similar for solar cycles 21 and 22 and so argued that the drift in average open flux values found by the near-Earth methods is not correct and thus that the Ulysses result cannot be valid. We here show that although cycles 21 and 22 are indeed similar, the deductions of Arge et al. are incorrect. This paper presents a study of open flux estimates derived from the aa index $[F_S]_{aa}$, from IMF observations $[F_S]_{IMF}$, and from photospheric magnetograms via the PFSS procedure $[F_S]_{PFSS}$. The average open solar flux derived by all three methods is shown to have peaked between cycles 21 and 22, and the behavior of the long-term drift is very similar indeed for all three. We also show that observations of cosmic rays and cosmogenic isotopes strongly support the long-term drifts in open flux found on longer timescales.

2. Ulysses Result

2.1. Uncertainty in Open Flux Estimates

[9] Figure 1 summarizes the results of *Lockwood et al.* [2003], who have studied the uncertainties caused by

application of the Ulysses result. The dashed line in Figure 1 shows the percentage deviation of the distance-corrected modulus of the radial field seen at Ulysses $\{(r_U/R_1)^2|B_{rU}|\}$ from that observed by near-Earth satellites $|B_{r1}|$. These data are for the first perihelion pass, which took place between day 280 of 1994 and day 235 of 1995. The heliocentric distance of the craft r_U varied from about 2.3 AU at the highest latitudes to 1.34 AU at perihelion. The radial field seen by Ulysses has been corrected by the $(r_U/R_1)^2$ factor to allow for the dependence of flux tube area on heliocentric distance r. In addition, the time δt for the solar wind observed by Ulysses to have propagated from $r = R_1$ to the satellite at $r = r_U$ has been calculated from the solar wind speed observed at Ulysses: Ulysses magnetometer observations at time t_u are then compared with near-Earth IMF data recorded at time $(t_u - \delta t)$. Figure 1 shows the fractional r.m.s. deviation of the lagged, range-corrected, averaged radial field seen by Ulysses as a function of the averaging timescale employed, T. It can be seen that in daily values, the average deviation is almost 50%, but this falls to near 10% for 27-day averages as solar longitudinal structure is averaged out and converges with increasing T to an asymptotic limit (shown by the horizontal dashed line) of 7% for the entire pole-to-pole pass (which lasts almost twelve 27-day solar rotation periods). The mean deviation averages to zero for T > 27 days, and thus the uncertainty shown in Figure 1 is a random rather than a systematic error.

[10] However, this deviation is not the error in $[F_S]_{aa}$ and $[F_S]_{IMF}$, incurred by the use of equation (1). The total open flux is the integral of $\underline{B}.\underline{da}$ over a whole sphere (where $\underline{da}$ is a surface area element). For averaging intervals of duration T, this becomes the sum over $N_\phi = (\tau/T)$ solar longitude bins (each $\Delta\phi = 2\pi/N_\phi$ in extent) and $N_\lambda = (T_p/T)$ solar latitude bins (of roughly constant extent $\Delta\lambda = \pi/N_\lambda$), where τ is the solar rotation period and T_p is the duration of the pole-to-pole pass. Expressing the total open flux as a fraction of that deduced from equation (1), this yields

$$F_S/F'_S = (1/2\pi)\Sigma^{N_\phi}\ \Sigma^{N_\lambda}\ (r_U/R_1)^2\{|B_{rU}|/|B_{r1}|\}\cos\lambda\Delta\lambda\Delta\varphi. \quad (2)$$

[11] From equation (2) we can compute the effect of the uncertainty in $\{(r_U/R_1)^2|B_{rU}|/|B_{r1}|\}$ (given by the dotted line in Figure 1) in giving an uncertainty in (F_S/F'_S) and hence F'_S. The result, as a function of the averaging timescale T, is the solid line in Figure 1. The important result is that the error in F'_S is less than 5% for $T \geq 27$ days. *Lockwood et al.* [2003] also show that an almost identical result is obtained for the second perihelion pass of Ulysses which took place between day 353 of 2000 and day 301 of 2001. The mean sunspot numbers for these two passes were 23.5 and 106.5; thus it has been shown that the error in using equation (1) is <5% for $T \geq 27$ days, at both at sunspot minimum and at sunspot maximum.

2.2. Open Solar Flux From IMF Data

[12] Observations of the interplanetary magnetic field (IMF) have been made since 1963. The earlier data were intercalibrated into the homogeneous "Omnitape" data set of hourly data by *Couzens and King* [1986], and this has been extended with data for up to the present day. This data set gives the near-Earth heliospheric radial field component B_{r1} which can be used with equation (1) to give the open flux estimate $[F_S]_{IMF}$.

[13] Figure 2 shows that the open solar flux has not been constant for the past 3.5 sunspot cycles. For cycle 22 the maximum-to-minimum ratio in monthly averages is greater than 2. Furthermore, there are long-term trends in the data which are discussed in section 4. The vertical dashed lines give the times of the two perihelion passes of Ulysses. The horizontal dashed lines in the top panel show the total radial flux (integrated from pole-to-pole and r^2 corrected to R_1) seen by Ulysses during these passes, $[F_S]_{U1} = 4.12 \times 10^{14}$ and $[F_S]_{U2} = 4.36 \times 10^{14}$ Wb. As discussed in the previous section, these values agree with the simultaneous $[F_S]_{IMF}$ averages for the same intervals to within 5%. The horizontal dashed lines in the bottom panel show the mean sunspot numbers for these passes which were 23.5 and 106.5. Thus although the two Ulysses passes took place at very different sunspot numbers, they yielded similar open flux estimates. This is consistent with the time variation of $[F_S]_{IMF}$ shown, which reveals that cycle 23, like cycle 20, has a small amplitude variation but that cycles 21 and 22 showed larger variations.

2.3. The aa Geomagnetic Activity Index

[14] *Mayaud* [1972] devised the aa index to quantify geomagnetic activity from a data series that extend homogeneously and continuously back to 1868. On annual timescales the aa index is almost identical to other planetary indices of geomagnetic activity derived from a greater number of stations (for example the Ap index, which is available for 1936 onwards). The aa index is generated from measurements from stations in southern England and in Australia. The variation of the annual means of aa shows two striking features. The first is the expected solar cycle variation, and the second is a clear upward drift throughout the 20th century. *Clilverd et al.* [1998] made a comprehensive study of all the possible causes of this long-term drift and, by a process of elimination, concluded that it was caused by a variation in interplanetary space and thus the Sun.

[15] We get an indication of the solar origin of the drift if we consider how the aa index is derived. The range of horizontal perturbations to the geomagnetic field in every 3-hour interval is scaled and converted into an aa index for each hemisphere (aa_N and aa_S) using the station-dependent scaling procedure devised by *Mayaud* [1972]. Figure 3 presents the 20-year running means, $\langle aa_N\rangle_{20}$ and $\langle aa_S\rangle_{20}$ which show the long-term drift is present in both the Northern and Southern Hemisphere data and has an almost identical waveform in the two cases. However, the drift is consistently 16% larger in amplitude for the Northern Hemisphere. Figure 3 also gives the detrended solar cycle variations in annual means $\Delta aa_N = aa_N - \langle aa_N\rangle_{20}$ and $\Delta aa_S = aa_S - \langle aa_S\rangle_{20}$. The two show similar solar cycle variations. Figure 4 is a scatterplot of the Northern and Southern Hemisphere data, with the points being for the detrended solar cycle variations and the crosses being for the running means. The solid line is a best-fit linear regression to the 20-year means and has a slope of 1.16. This regression line also matches the detrended data well,

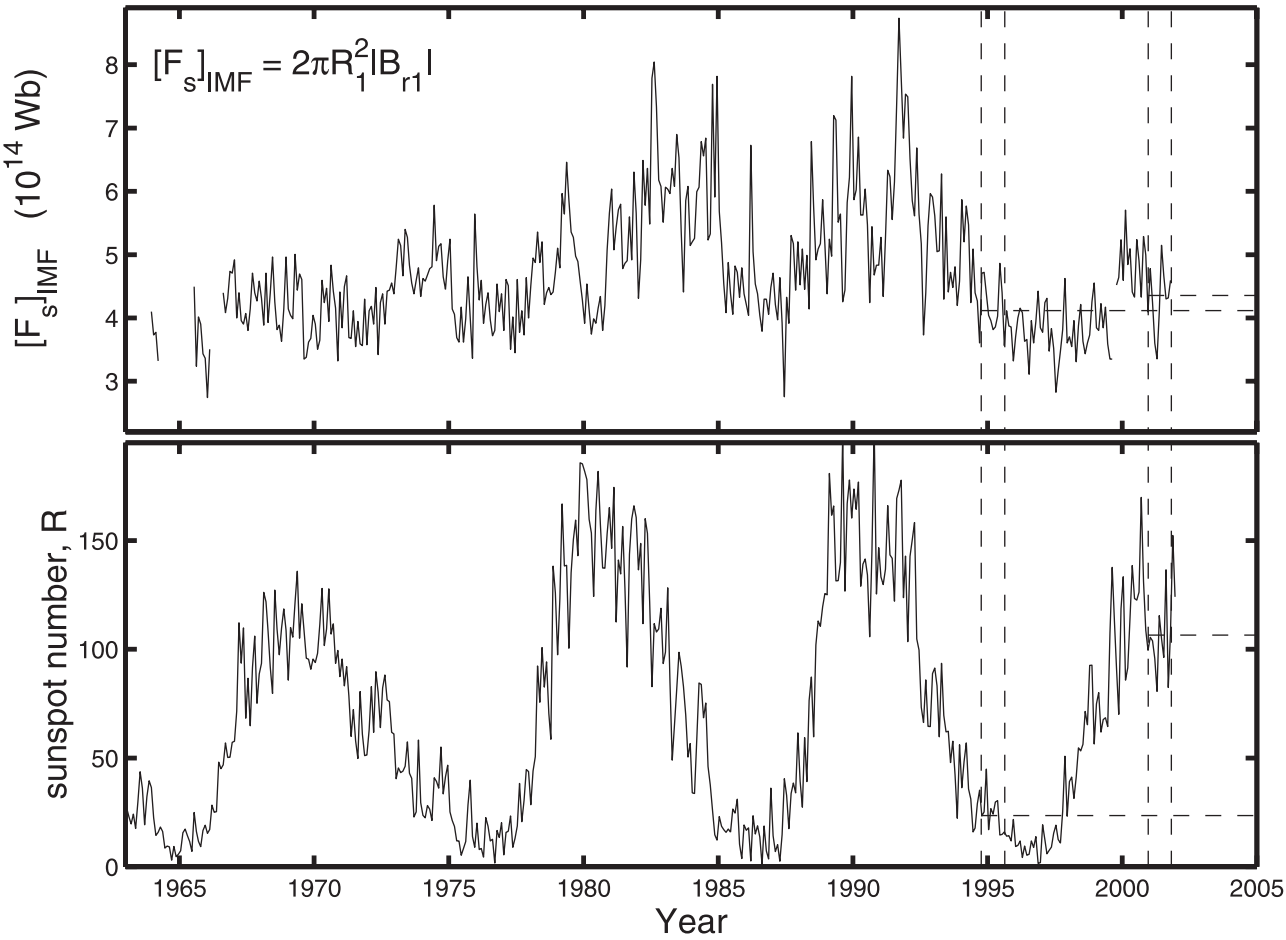

Figure 2. The variations monthly means (a) of the open solar flux deduced from interplanetary magnetic field (IMF) observations $[F_s]_{IMF} = 2\pi {R_1}^2 |B_{r1}|$ (where R_1= 1AU and B_{r1} is the near-Earth radial component of the IMF) and (b) of the sunspot number R. The vertical dashed lines mark the fast latitude scans of the first and second perihelion passes of Ulysses. The horizontal dashed lines in each panel show the mean values during these passes.

i.e., the solar cycle variation also shows the Northern Hemisphere data to be consistently 16% larger in amplitude than the Southern. If the scaling factors (for converting the ranges observed at the two stations into hemispheric aa indices) were perfect, this regression fit would be the dotted line of slope 1 shown in Figure 4. The fact that both the solar cycle variation and the long-term drift lie on the same line strongly suggests that the long-term drift and the solar cycle share the same cause, i.e., the Sun. This also confirms *Clilverd et al.*'s [1998] elimination of several possibilities that would have influenced the ratio of the station-dependent scaling factors. For example, the change in Earth's magnetic axis has caused drifts in the geomagnetic latitudes of the Northern and Southern Hemisphere stations which are in opposite directions. The conclusion that the drift is due to a solar effect is confirmed and quantified by the analysis of *Stamper et al.* [1999] and *Lockwood et al.* [1999a], discussed in the next section.

2.4. Open Solar Flux From Geomagnetic Activity

[16] *Lockwood et al.* [1999a] have presented a method for computing the radial component of the near-Earth IMF from annual means of the aa geomagnetic activity index (aa = $[aa_N + aa_S]/2$). The Ulysses result can then be applied, as in section 2.2, to give the open flux variation over the longer period covered by homogeneous observations of geomagnetic activity.

[17] A description of the procedure to derive the open flux values $[F_S]_{aa}$ has been given previously [*Lockwood et al.*, 1999a, 1999b; *Lockwood and Stamper*, 1999] and will not be repeated here. However, there are some important points to stress because the method is physics-based and is far from being a simple statistical extrapolation using a fit to the aa index. First, it is based on the theory of solar wind magnetosphere energy coupling by *Vasyliunas et al.* [1982], which has been shown to be the most successful by I. Finch, M. Lockwood, and R. Stamper (Solar wind-magnetosphere coupling functions on timescales of 1 day to 1 year, submitted to *Annales Geophysicae*, 2003), giving a correlation of 0.97 between interplanetary parameters and the aa index on annual timescales. Second, it employs the Parker spiral theory to the ecliptic heliospheric field which, on the annual timescales used, matches the data exceptionally well [*Gazis*, 1996; *Stamper et al.*, 1999]. Third, the method exploits our understanding of the role of fast solar wind streams (from long-lived, low-latitude coronal holes) in generating recurrent geomagnetic activity [*Cliver et al.*, 1996; *Hapgood*, 1993] this enables us to remove the effect

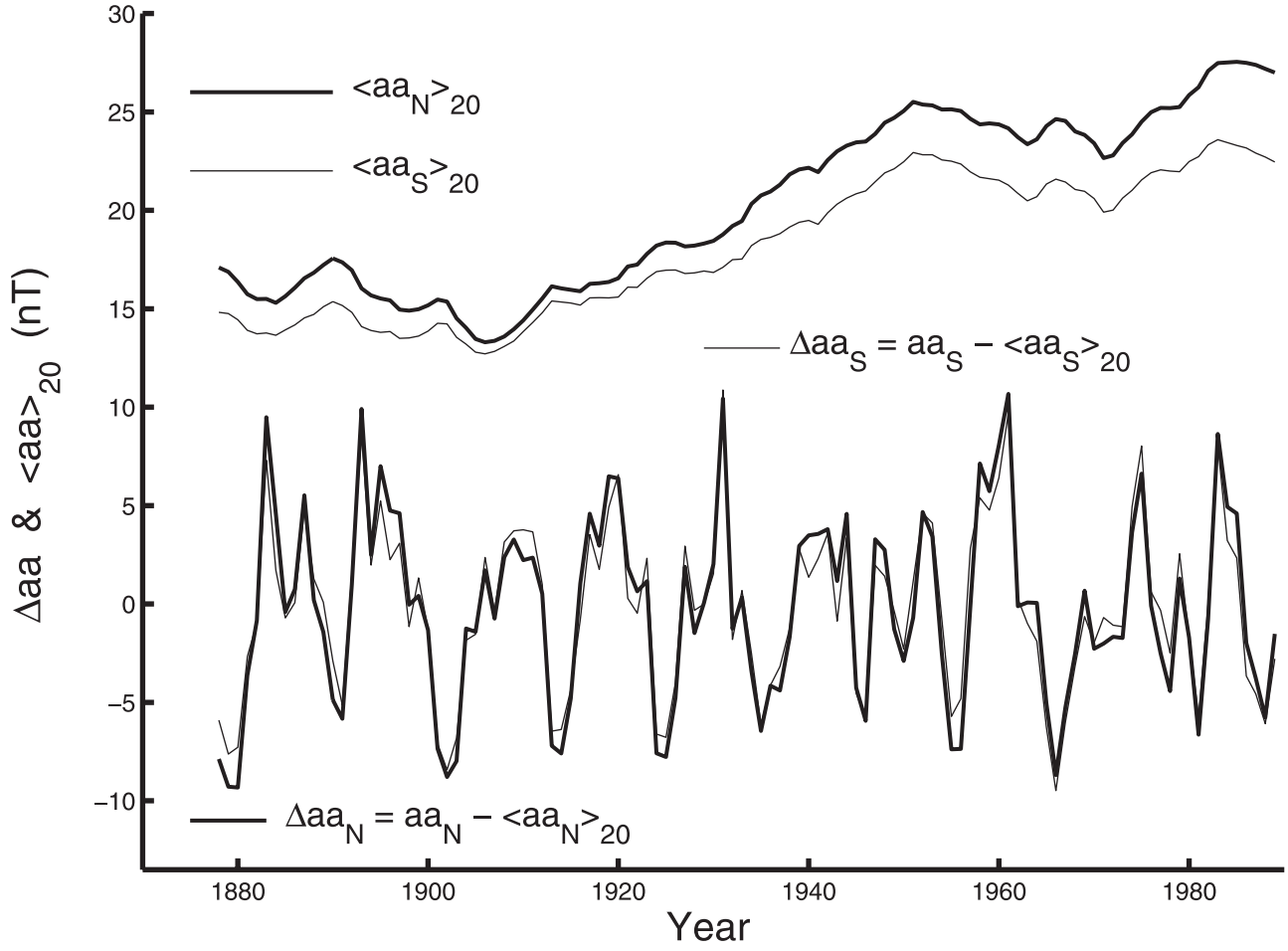

Figure 3. The aa indices from the Northern (thick lines) and Southern (thin lines) Hemispheres. The top pair of lines are 20-year running means, $\langle aa_N \rangle_{20}$ and $\langle aa_S \rangle_{20}$, revealing the long-term drifts in both the northern and southern data sets. The lower curves show the detrended solar cycle variations in annual means $\Delta aa_N = aa_N - \langle aa_N \rangle_{20}$ and $\Delta aa_S = aa_S - \langle aa_S \rangle_{20}$.

of solar wind velocity variations. The three correlations used to generate the required coefficients are all over 0.95 and are all more than 99.999% significant, allowing for the persistence in the various data series.

[18] The method of *Lockwood et al.* [1999a, 1999b] is applied to 12-month intervals to eliminate annual effects (such as the annual variation in the Earth-Sun distance and the Earth's dipole tilt) and seasonal effects (such as the variation of ionospheric conductivity around the aa magnetometer sites). These 12-month intervals are advanced one month at a time to produce monthly data, but only every twelfth estimate is fully independent. The resulting $[F_S]_{aa}$ estimates for 1993–2001 are shown by the grey shaded area in Figure 5a and compared with annual means of the open flux from the near-Earth IMF observations ($[F_S]_{IMF}$, solid line). It can be seen that agreement is very good especially considering that only data from 1976–1993 were used in deriving the coefficients required.

[19] Rows 1 and 2 of Table 1 list details of the correlation between $[F_S]_{aa}$ and $[F_S]_{IMF}$. For the monthly data (row 2), the best fit was obtained with a lag L between the two data series of Zero. (Using the Fisher-Z test for the significance of a difference between two correlation coefficients, we find that at the 90% confidence level L is between −7 and +4 months). The $N = 415$ pairs of data points at this L give a correlation coefficient $c = 0.639$, which means that the fraction of the variation in $[F_S]_{IMF}$ "explained" (in a statistical sense) by $[F_S]_{aa}$ is $c^2 = 0.41$. The RMS deviation of $[F_S]_{IMF}$ from $[F_S]_{aa}$ is $[\Delta F_S]_{RMS} = 6.28 \times 10^{13}$ Wb.

[20] In order to compute the statistical significance of this correlation, we must allow for the "persistence" or "conservation" in the data. We can quantify the significance using the Student's t-test, but only after making a correction to the number of degrees of freedom to allow for persistence [*Wilks*, 1995]:

$$N_e = N(1 - a_1)/(1 + a_1), \tag{3}$$

$$t = |c|\{(N_e - 2)/(1 - c)\}^{1/2}, \tag{4}$$

where N is the number of samples, N_e is the effective number of samples, and a_1 is the mean autocorrelation at lag 1 of the two data series, which are 0.687 for $[F_S]_{IMF}$ and 0.873 for $[F_S]_{aa}$. This yields $N_e = 51.2$, a t statistic of $t =$

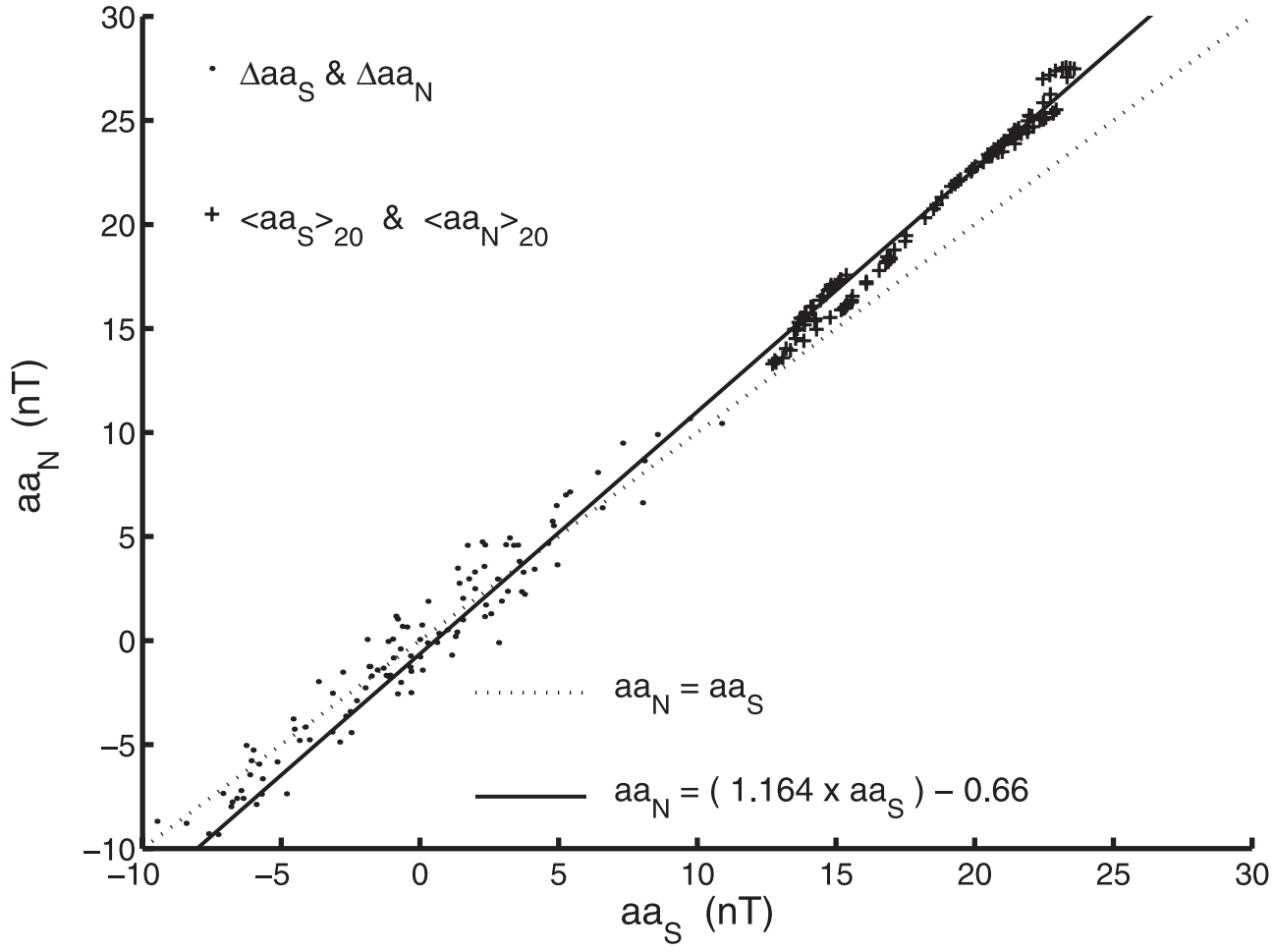

Figure 4. Scatterplots of the aa indices from the Northern and Southern Hemispheres. The crosses are for 20-year running means, $\langle aa_N \rangle_{20}$ and $\langle aa_S \rangle_{20}$. The points are for the detrended annual means, $\Delta aa_N = aa_N - \langle aa_N \rangle_{20}$ and $\Delta aa_S = aa_S - \langle aa_S \rangle_{20}$. The solid line is the best fit to the 20-year means.

5.82, and a significance level of $S = \{100 - (2.2 \times 10^{-5})\}\%$ (i.e., the probability that this result was a chance occurrence is 2.2×10^{-7}).

[21] Row 1 of Table 1 gives the corresponding analysis of the correlation between annual means of $[F_S]_{IMF}$ and $[F_S]_{aa}$. The correlation coefficient is raised to $c = 0.866$ ($c^2 = 0.75$), but the lower number of samples ($N = 37$) means the significance is lowered slightly to $S = 99.7\%$ (the probability of this being found by chance is 0.003).

2.5. Comparisons With Results From the PFSS Method

[22] We here make use of the open flux estimates $[F_S]_{PFSS}$ produced using the PFSS method by *Wang and Sheeley* [2002]. These authors give full details of the original magnetogram data used, of the Ulrich correction applied for line saturation, and of the implementation of the PFSS method. The solid line in Figure 5b gives monthly means of these $[F_S]_{PFSS}$ data and allows comparison with the variation derived from the aa index, $[F_S]_{aa}$. Values of $[F_S]_{PFSS}$ are derived once every Carrington rotation period and these have been linearly interpolated into monthly data to allow correlations with $[F_S]_{aa}$. Agreement is again good, which is to be expected because *Wang and Sheeley* showed that there was good agreement between the radial field values deduced from the PFSS method with those measured in near-Earth interplanetary space (their Figure 1).

[23] Comparison of Figures 5a and 5b shows that the agreement between the open flux variations derived from aa and the PFSS procedure ($[F_s]_{aa}$ and $[F_s]_{PFSS}$) is not quite as close as for $[F_s]_{aa}$ and $[F_s]_{IMF}$. This is confirmed by rows 3 and 4 of Table 1 which show that the correlation coefficients are 0.567 and 0.703 for monthly and annual data, respectively (significance levels 99.5% and 94.5%).

3. Galactic Cosmic Rays and the Open Solar Flux

[24] The heliosphere shields the Earth from the galactic cosmic rays. The contributions of various mechanisms for deflecting cosmic rays is a matter of debate, as is the part of the heliosphere where most of the shielding takes place [e.g., *Jokipii*, 1991; *McCracken and McDonald*, 2001]. Irregularities in the heliospheric field scatter the cosmic rays and the occurrence and amplitude of these irregularities, and the consequent merged diffusive barrier presented to cosmic rays, increases with the magnitude of the heliospheric field and thus with the total open solar flux. *Cane et al.* [1999] show that most of the variation of the cosmic ray

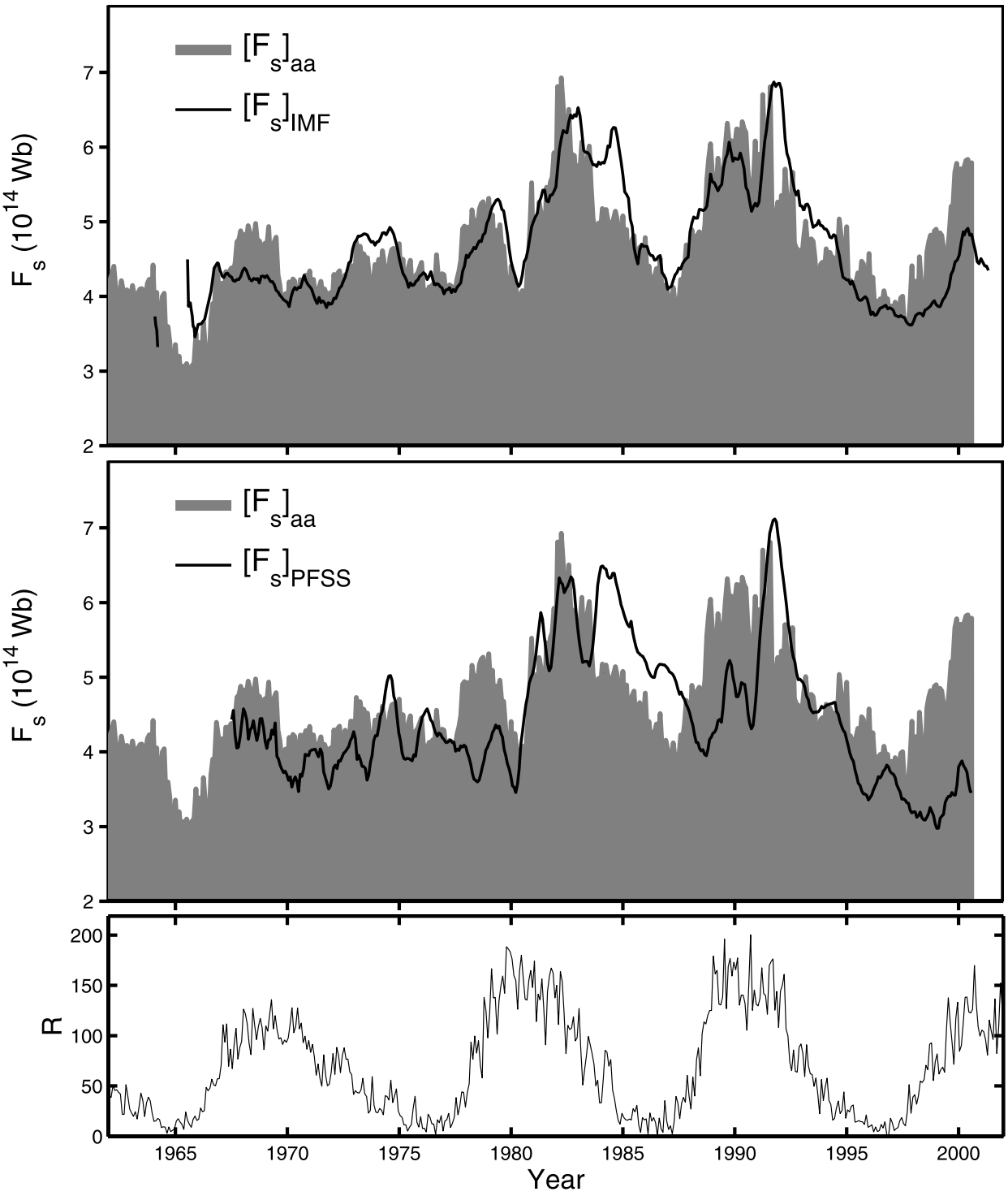

Figure 5. Variations for 1963–2001 of (a) the monthly open flux estimates derived from 12-month intervals of the aa index ($[F_s]_{aa}$, grey shaded area) and 12-point running means of monthly data derived from the IMF ($[F_s]_{IMF}$ black line); (b) the same as Figure 5a but for open flux estimates derived from photospheric magnetograms using the PFSS method ($[F_s]_{PFSS}$, black line); (c) the monthly means of the sunspot number, *R*. Details of the correlations are given in Table 1.

fluxes is "explained" (in a statistical sense) by the strength of the heliospheric field: the tilt angle of the heliospheric current sheet is a discernible additional factor only close to sunspot minimum and this, in turn, correlates well with the solar cycle variation in the open flux. For these reasons the flux of cosmic rays anticorrelates strongly with the open flux. *Lockwood* [2001] found that cosmic ray fluxes observed by various neutron monitors around the globe

Table 1. Details of Correlations

	Dates	Data Resolution	Correlation Coefficient, c	c^2	Number of Pairs of Data Points, N	Mean ACF at Lag 1, ρ_1	RMS Deviation from Best Fit, Δ_{RMS}, 10^{14} Wb	Lag, L, months	Significance, S, %
Radial IMF, $[F_S]_{IMF}$ & $[F_S]_{aa}$	1963–2000	annual	0.866	0.75	37	0.65	0.369	0 ± 6	99.72
Radial IMF, $[F_S]_{IMF}$ & $[F_S]_{aa}$	1963.8–2000	monthly	0.639	0.41	415	0.78	0.628	$-7 \le L \le 4$	$100 - (2.2 \times 10^{-5})$
PFSS method, $[F_S]_{PFSS}$ & $[F_S]_{aa}$	1970–2000	annual	0.703	0.49	31	0.66	0.711	3 ± 3	94.5
PFSS method, $[F_S]_{PFSS}$ & $[F_S]_{aa}$	1969.3–2000.1	monthly	0.567	0.32	370	0.90	1.008	4 ± 4	99.50
Climax n.m. C & $[F_S]_{aa}$	1953–1999	annual	−0.836	0.70	46	0.73	0.400	0 ± 6	99.11
Climax n.m. C & $[F_S]_{aa}$	1953.8–2000.0	monthly	−0.784	0.62	556	0.94	0.527	0 ± 4	99.996
Huancayo/Hawaii n.m., H & $[F_S]_{aa}$	1953–1993	annual	−0.874	0.76	40	0.73	0.373	0 ± 6	98.96
Huancayo/Hawaii n.m., H & $[F_S]_{aa}$	1953.8–2000.0	monthly	−0.777	0.60	556	0.92	0.537	0 ± 4	99.9993
Moscow n.m. H & $[F_S]_{aa}$	1953–1993	annual	−0.874	0.76	40	0.73	0.373	0 ± 6	98.96
Moscow n.m. H & $[F_S]_{aa}$	1958.8–2000	monthly	−0.782	0.61	496	0.93	0.521	$-1 \le L \le 8$	99.99
Ion chambers C_{ic}[a] & $[F_S]_{aa}$	1954–1994	annual	−0.879	0.77	40	0.71	0.365	0 ± 6	99.52
Ion chambers C_{ic}[b] & $[F_S]_{aa}$	1937–1994	annual	−0.839	0.70	57	0.68	0.375	0 ± 6	99.93
Forbush data F & $[F_S]_{aa}$	1937–1958	annual	−0.817	0.67	21	0.35	0.340	0 ± 6	99.81
Neher data N & $[F_S]_{aa}$	1936–1958	annual	−0.902	0.81	7	0.11	0.308	0 ± 6	99.16

[a]Excludes Cheltenham data.
[b]Includes Cheltenham data.

are strongly and significantly anticorrelated with the open flux, as deduced from the aa index. Because the shielding of the cosmic rays takes place throughout the heliosphere, the anticorrelation with near-Earth open flux estimates is of relevance Ulysses result concerning the uniformity of the radial field.

[25] The quality of the anticorrelation between cosmic ray fluxes and the open solar flux is demonstrated by Figure 6. The cosmic ray data are monthly means of the count rates H from the neutron monitors in Huancayo and Hawaii. Together, these two stations provide a continuous and homogeneous data sequence, with the data series being continued at Haleakala, Hawaii after monitoring ceased at Huancayo, Peru in 1993. For these stations, primary cosmic rays of rigidity exceeding a geomagnetic cut-off of 13.45GV are detected. Very similar results are obtained for other stations with different rigidity cut-offs. In Figure 6 the count rate H has been scaled to give an open solar flux estimate $[F_S]_H$ using a best fit linear regression to $[F_S]_{aa}$.

[26] This best fit between $[F_S]_{aa}$ and H for monthly data was obtained with a lag of $L = 0$ (and between −4 and +4 months at the 90% confidence level). The correlation coefficient is $c = -0.777$, which means that the fraction of the cosmic ray variation "explained" (in a statistical sense) by the open flux variation is $c^2 = 0.61$. The significance level of this correlation is $S = 99.9993\%$. For annual means, these figures become $c = -0.874$, $c^2 = 0.76$, and $S = 98.96\%$. These values are very similar to those for other neutron monitors: Table 1 also gives the values for the long data sequences from Climax and Moscow (geomagnetic rigidity cut-offs of, respectively, 3.03 GV and 2.46 GV).

[27] The lag is $L < 4$ months and, for a fast, polar solar wind speed of $V_{sw} = 600$ kms^{-1}, this implies that most of the cosmic ray shielding is at $r < LV_{sw} \approx 84$ AU.

[28] Near sunspot minima the cosmic ray flux variation H shows the characteristic alternate peaked and flat-topped maxima (seen as the corresponding minima in $[F_S]_H$ in Figure 6) [*Ahluwalia*, 1997]. This effect is often ascribed to polarity-dependent drifts of the cosmic rays in the heliosphere [*Jokipii*, 1991]. However, Figure 6 shows that this behavior is also seen in the open flux values $[F_S]_{aa}$. Thus this 22-year cycle appears to be caused by a variation in the open heliospheric flux and not to be a property of the expected polarity-dependent drifts of the cosmic rays within the heliosphere.

[29] Table 1 and Figure 6 confirm that a linear relationship between the cosmic ray fluxes and the open solar flux has applied since 1953. However, this does not take us back to cycles before 19 when the major change in open flux reported by *Lockwood et al.* [1999a, 1999b] occurred. The data from another type of cosmic ray monitor, namely ionization chambers, does cover a slightly longer period. The variation in these data, again scaled using a linear regression with the open flux derived from aa, is shown in Figure 7. The grey shaded area gives annual means of $[F_S]_{aa}$, and the solid line shows the scaled variation $[F_S]_{ic}$ from the Fredricksberg and Yakutst detectors which are well intercalibrated.

[30] The dashed line in Figure 7 shows the scaled variation $[F_S]_F$ from Forbush's original data, as presented by *McCracken and McDonald* [2001]. These data were taken by a network of 5 "Carnegie Type C" ionization chambers established in 1936–1967 which were monitored closely and corrected for sensitivity changes [*Forbush*, 1958]. McCracken and McDonald point out that Forbush's data show a downward drift in average cosmic ray fluxes between 1936 and 1958, consistent with the downward drift in ^{10}Be isotope abundances at this time. This drift is sometimes suppressed by recalibrations of the data which effectively assume that it is instrumental in origin; it appears as an upward drift in $[F_S]_F$ in Figure 7, consistent with the open flux variation deduced from aa. In addition, *Neher et al.* [1953] made observations from high altitude ionization chambers from 1933 to 1965. The intercalibration of the instruments was quoted as being better than 1%. These data, scaled using a linear regression to give $[F_S]_N$, are shown by the stars in Figure 7. Both of these early cosmic ray data sets are, like the later observations from both neutron monitors and ionisation chambers, entirely consistent with the open

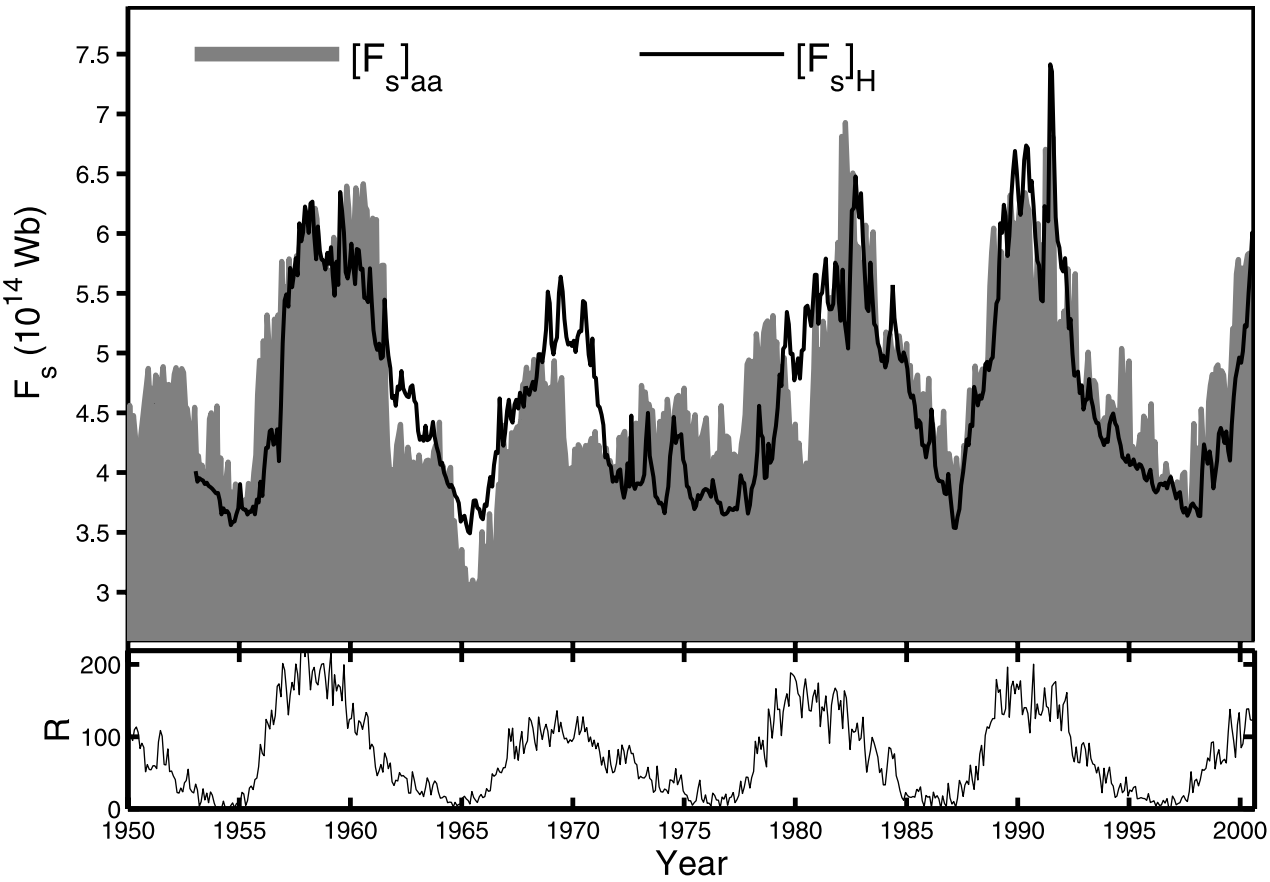

Figure 6. Variations of (a) the monthly open flux estimates derived from 12-month intervals of the aa index ($[F_s]_{aa}$, grey shaded area) and monthly means of the cosmic ray counts H observed at Huancauyo and Hawaii (scaled using a linear regression with $[F_s]_{aa}$ to give $[F_s]_H$, shown by the black line); and (b) the monthly means of the sunspot number, R. Details of the correlations are given in Table 1.

solar flux variation deduced from the aa index. The r.m.s. differences between $[F_S]_{aa}$ and open fluxes scaled from cosmic ray counts are the same magnitude as the r.m.s. differences between those scaled for different cosmic ray observation sites. Thus the cosmic ray observations provide strong support for the long-term variation in the open solar flux computed from the aa index. Table 1 shows that c^2 = 70–80% of the variation in annual means of cosmic ray fluxes is accounted for by the variation in $[F_S]_{aa}$. By comparison, 75% of the variation in the open flux deduced from IMF observations is explained by the variation deduced from aa. Part of the ''unexplained'' variation in the cosmic ray fluxes will be due to the uncertainties of the method, including the 5% introduced by the use of the Ulysses result (see section 2.1).

4. Long-Term Variation of the Open Solar Flux

[31] Figure 8 shows the full sequence of $[F_S]_{aa}$ values since 1868 (area shaded grey) [*Lockwood et al.*, 1999a, 1999b] with the $[F_S]_{IMF}$ values for after 1963 added as a black line (see Figure 5a for a more detailed comparison). The main features are a solar cycle variation superposed on a long-term drift that has been predominantly upward since 1900.

[32] In order to quantify this long-term drift, Figure 9 shows 11-year running means of the open solar flux. Values derived from aa, $\langle[F_S]_{aa}\rangle_{11}$, reveal that (1) the average open flux increased by 2.17 between 1900 and 1987 and (2) this factor was 1.29 for 1967–1987. The latter rise of 29% is similar to that quoted by *Lockwood et al.* [1999a] from a linear fit to $[F_S]_{IMF}$ for three full solar cycles (20, 21, and 22). The 11-year running means from the IMF data, $\langle[F_S]_{IMF}\rangle_{11}$, are shown by the solid line. The most recent data show that the downturn, seen by Lockwood et al. near the end of the data sequence available to them, has subsequently continued. As a result, 1987 can now be seen to have been a significant peak (marked by the vertical arrow). Figure 9 also shows that the 11-year means of the sunspot number, R_{11}, has followed a similar curve. Other terrestrial data, such as the occurrence of low-latitude aurorae [*Pulkkinen et al.*, 2001], as well as other solar data, such as the latitudinal spread of sunspots [*Foster and Lockwood*, 2001] also show very similar variations on both solar cycle and 100-year timescales.

[33] Figure 10 shows the variation in $\langle[F_S]_{aa}\rangle_{11}$ over the last three solar cycles in more detail. Also shown are $\langle[F_S]_{IMF}\rangle_{11}$ and the corresponding 11-year running means of open flux from the PFSS model, $\langle[F_S]_{PFSS}\rangle_{11}$. It can be seen that the long-term drift in the open flux from all three methods is very similar with, in all three cases, a consistent rise before a peak in 1987 and a subsequent fall. The drifts in $\langle[F_S]_{IMF}\rangle_{11}$ are very similar indeed to those in $\langle[F_S]_{aa}\rangle_{11}$;

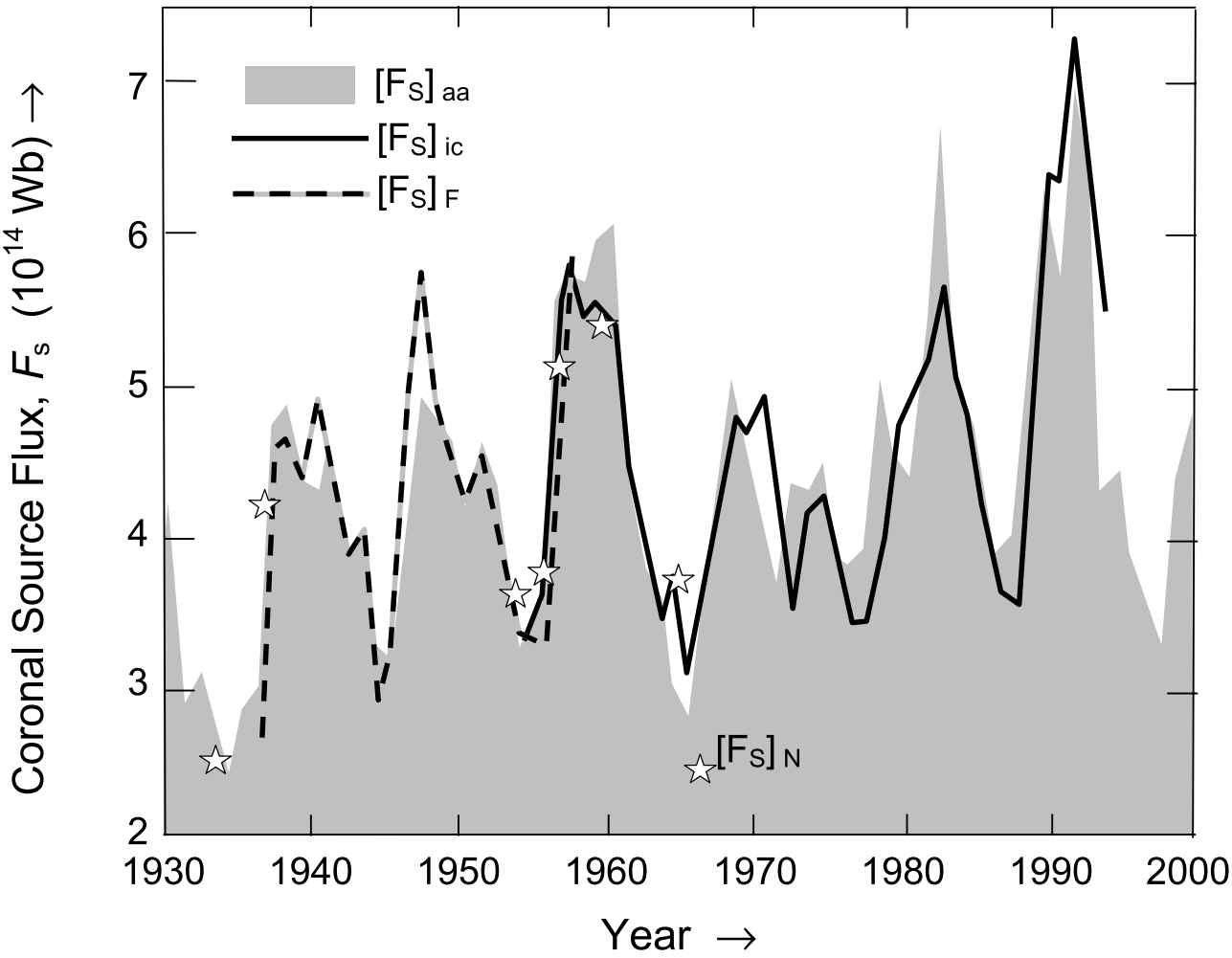

Figure 7. Annual means of the open solar flux from the aa index (grey shaded area) compared with the variations of cosmic ray fluxes observed by a variety of ionization chambers, scaled using linear regression fits with $[F_s]_{aa}$. The solid line is the variation deduced from the data from the Fredricksberg and Yakutst instruments, $[F_s]_{ic}$. The dashed line shows the variation scaled from Forbush's original data $[F_s]_F$ and the stars are from Neher's data $[F_s]_N$. Details of the correlations are given in Table 1.

those in $\langle[F_S]_{PFSS}\rangle_{11}$ are similar but consistently somewhat larger in amplitude.

[34] Figure 10 also shows the long-term variation in $\langle[F_S]_M\rangle_{11}$, the open flux derived from a linear regression fit between the cosmic ray counts M detected by the Moscow neutron monitor and $[F_S]_{aa}$. The long-term drifts in the scaled cosmic ray data are very similar indeed to those in $\langle[F_S]_{aa}\rangle_{11}$, $\langle[F_S]_{IMF}\rangle_{11}$, and $\langle[F_S]_{PFSS}\rangle_{11}$. We conclude that for the three solar cycles for which comparisons are possible, the drift in average open solar flux deduced from aa is very similar, in both variation and amplitude, to the drifts deduced from both IMF and photospheric observations. This is also mirrored by the long-term drift in average cosmic ray fluxes over the same period.

5. Model of the Long-Term Variation of the Open Solar Flux

[35] The open magnetic flux mainly emerges through the photosphere in active regions [*Harvey and Zwaan*, 1993] and is the moved around by meridional circulation, differ-

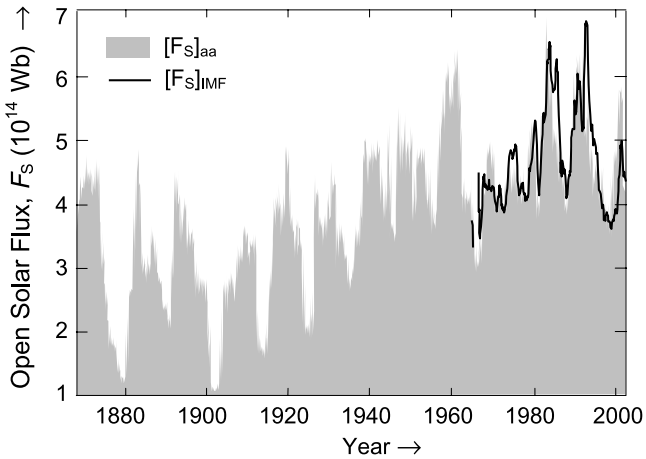

Figure 8. The variations of open solar flux. The area shaded grey gives values for 1 year (advanced by 1 month at a time) derived from the aa geomagnetic index, $[F_s]_{aa}$; the black solid line gives monthly values from IMF observations $[F_s]_{IMF}$ (shown in more detail in Figure 5a).

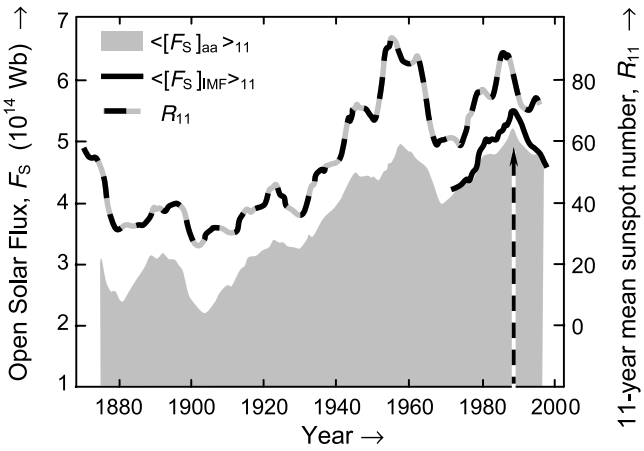

Figure 9. Long-term variations in 11-year running means. The area shaded grey gives the 11-year running averages of the open solar flux derived from the aa index, $\langle[F_s]_{aa}\rangle_{11}$; the black solid line gives the corresponding values derived from IMF observations $\langle[F_s]_{IMF}\rangle_{11}$. The dashed line is the average sunspot number, R_{11}, and the vertical arrow marks the peak value seen in 1987.

ential rotation, and diffusion [*Wang et al.*, 2000a; *MacKay et al.*, 2002a, 2002b]. *Solanki et al.* [2000, 2002] have devised a simple model of the open flux variation. This model is not concerned with how the open flux is distributed over the solar surface; rather it deals with the continuity equation of the total amount. The total production (emergence) rate is quantified from a semiempirical function of sunspot number. The loss rate is assumed to be linear, with a loss time constant that is found from the best fit to the data of *Lockwood et al.* [1999a, 1999b] to be 3.6 years. In Figure 11, the dashed line shows the model prediction obtained by running the model forward from an initial open flux that is taken to be zero at the end of the Maunder minimum. The model reproduces the behavior noted by *Lockwood* [2001], in that longer solar cycles allow the open flux to decay away to a greater extent whereas a series of shorter cycles causes an accumulation of the open flux.

[36] This model was devised in 1999 to match the open flux variation in the available data, which at that time was for 1868–1996. Thus the good fit ensures that the model matches well the average open flux seen during the first perihelion pass of Ulysses, $[F_S]_{U1}$. Subsequently, the model has matched the evolution of the open flux well and has

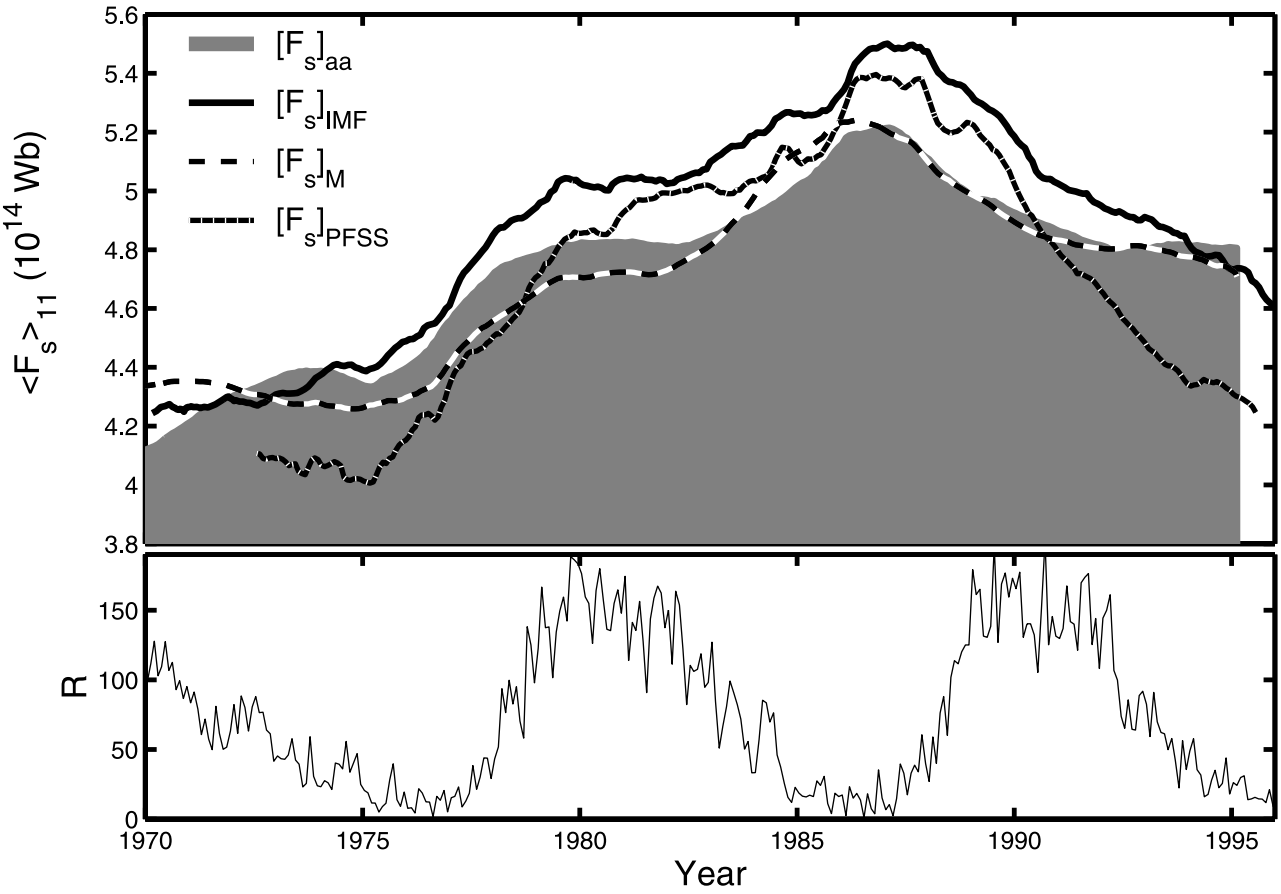

Figure 10. (a) Variations of 11-year means of open flux estimates derived by various methods for 1970–1996: The area shaded grey gives values from the aa index $\langle[F_s]_{aa}\rangle_{11}$, the black solid line gives values derived from IMF observations $\langle[F_s]_{IMF}\rangle_{11}$, the dotted black and white line gives values from the PFSS method $\langle[F_s]_{PFSS}\rangle_{11}$, and the dashed black and white line gives values scaled from the cosmic ray counts detected by the Moscow neutron monitor $\langle[F_s]_{M}\rangle_{11}$. (b) The monthly means of the sunspot number, R.

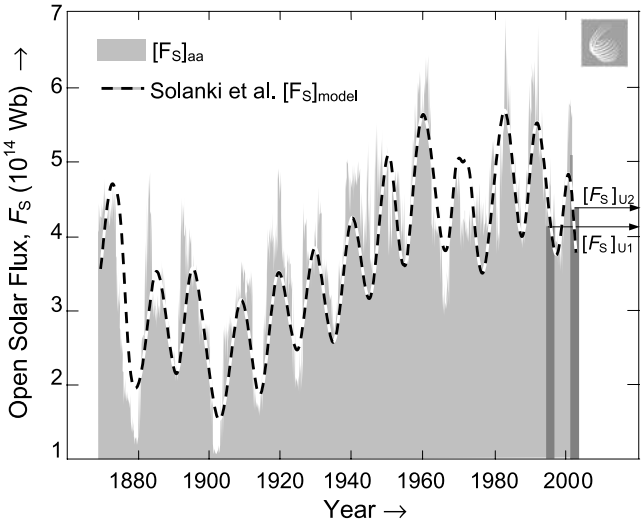

Figure 11. Observed and modelled variations of open solar flux. The area shaded grey gives the values derived from the aa index $[F_s]_{aa}$, as in Figure 8, and the dashed line is the prediction of the model by *Solanki et al.* [2000], $[F_s]_{model}$. The vertical dark grey bars give the intervals of the two perihelion passes of Ulysses, which yielded average open fluxes of $[F_s]_{U1}$ and $[F_s]_{U2}$, which are given by the horizontal arrows.

correctly predicted the open flux seen by Ulysses during its second perihelion pass, $[F_S]_{U2}$ (see Figure 11). Thus the model correctly reproduces the fact that the open flux near the peak of cycle 23 is only slightly larger than just before the preceding minimum, as was measured by Ulysses. This is because the cycle 23 has been a weaker cycle than its two predecessors (in terms of both sunspot number and flux emergence rate), because the Ulysses pass happened to be during a relative minimum between two peaks in the solar activity and also because the 11-year oscillation in open flux has been superposed on the downward trend that began in 1987 (see section 4).

6. Comparison With Cosmogenic Isotopes

[37] The modeled variation of the open flux can be tested on longer timescales using records of the abundance of the cosmogenic isotopes ^{10}Be and ^{14}C found in ice sheets and tree rings, respectively [*O'Brien*, 1979; *Beer et al.*, 1990; *Bard et al.*, 1997; *Beer*, 2000]. Section 3 discusses the strong anticorrelation of the open solar flux with the flux of galactic cosmic rays detected by a number of ground-based monitors. *Lockwood* [2001] has shown that there is also a significant anticorrelation between the open flux derived from aa and the abundance of the ^{10}Be isotope produced by cosmic rays impacting upon oxygen and nitrogen nucleii in the atmosphere (with a time lag of about 1 year which is predominantly due to the time for deposition into the ice sheet). This can be seen in Figure 12, in which the ^{10}Be abundance from the Dye-3 Greenland ice core [*Beer et al.*, 1990, 1998] has been scaled in terms of the open flux using the best fit linear regression (thin line). The open flux derived from the aa index $[F_S]_{aa}$ is shown by the thicker solid line: this sequence has here been extended back to 1844 using data from the Helsinki magnetometer [*Nevanlinna and Kataja*, 1993]. Very good agreement can be seen between the trends in the derived open flux and in the ^{10}Be abundance, with a broad minimum around 1890, a significant rise during 1900–1960, and a subsequent fall and then rise. Thus the ^{10}Be data provide very strong support for the long-term open flux variation found from the aa index.

[38] Figure 12 also shows, as the grey shaded curve, the open flux predicted by the model of *Solanki et al.* [2000]. In this case the model has been applied slightly differently; instead of running the continuity equation forward in time from an assumed open flux of zero at the end of the Maunder minimum (as was done by Solanki et al. and in Figure 11), it has here been run backward in time, starting from the observed open flux at the minimum between solar cycles 22 and 23. This yields a predicted total open flux of about 1×10^{14} Wb for 1705, at the end of the Maunder minimum. This is roughly a quarter of average present-day values (Figure 12). A similar value was derived from the linear regression of $[F_S]_{aa}$ with the ^{10}Be abundances by *Lockwood* [2001], as can be seen by the good agreement between the model and the open flux scaled from the ^{10}Be abundances in Figure 12.

[39] In addition, Figure 12 shows the results of a best fit to the production rate of the ^{14}C cosmogenic isotope, deduced from a two-reservoir model that allows for exchange between the atmosphere and the oceans and the biomass reservoirs [*Stuiver and Quay*, 1980]. The exchange with the biomass does not allow the 11-year cycles to be seen, and the data after the first man-made nuclear explosions cannot be used. Nevertheless, the results, shown by the dashed line, agree well with the long-term variations of the average open flux deduced from aa, from the ^{10}Be abundance, and by the model. Other cosmogenic isotopes, for example, ^{44}Ti found in meteorites also indicate the long-term drift over the 20th century [*Bonino et al.*, 1998].

7. Discussion and Conclusions

[40] Table 1 shows that strong and highly significant correlations exist between the open flux estimates derived from the three methods discussed here, namely from the aa geomagnetic index, from radial IMF observations, and from photospheric magnetograms using the PFSS method. The first two of these methods assume the Ulysses result that the radial field is independent of latitude. The 11-year running means shown in Figure 10 remove the solar cycle variations and reveal the long-term (>11 year) drifts in these data. The drifts are similar in all three cases and are actually slightly greater in the PFSS data than from the near-Earth estimates.

[41] All three methods reveal that the average open solar flux peaked near 1987, which is close to the solar minimum between cycles 21 and 22. Thus, as pointed out by *Arge et al.* [2002], averages over cycles 21 and 22 (defined from minimum to minimum) are similar. However, this does not mean that there are no long-term drifts. *Wang and Sheeley* [2002] point out that the average open fluxes, deduced from the PFSS method and from IMF observations, are greater in cycles 21 and 22 than in cycles 20 and 23; this is fully consistent with the results presented here and in very good agreement with the results using the aa geomagnetic index.

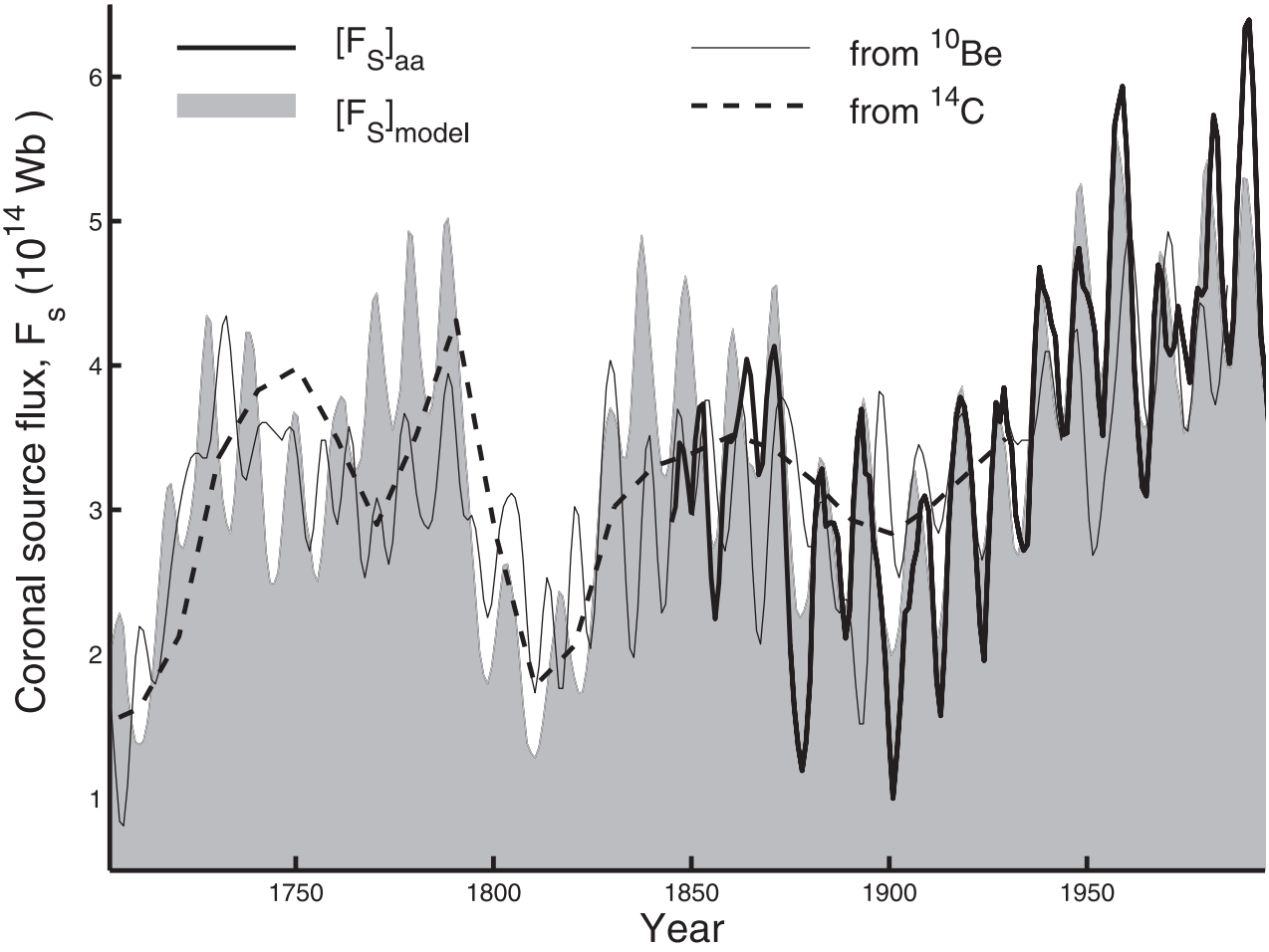

Figure 12. Modeled, observed, and inferred variations of the open flux since the end of the Maunder minimum. The area shaded grey gives the predictions of the model by *Solanki et al.* [2000], $[F_s]_{model}$. The thick solid line is the variation derived from the aa index $[F_s]_{aa}$, including the ''Helsinki extension'' data prior to 1868. The thin solid line is the abundance of the ^{10}Be isotope, as found in the Dye3 Greenland ice core and scaled as a function of open flux using a best fit linear regression [*Lockwood*, 2001a]. The dashed line gives the production rate of the ^{14}C isotope, also scaled as a function of open flux using a best fit linear regression: the production rate is determined from the isotope abundance in tree rings using a two-reservoir (oceans and biomass) model.

We conclude that the photospheric data support the drifts in the open flux deduced by *Lockwood et al.* [1999a, 1999b].

[42] *Arge et al.* [2002] argue that the near-Earth estimates of the open flux ($[F_S]_{aa}$ and $[F_S]_{IMF}$) show a drift only because the Ulysses result is not valid on long timescales. They therefore argue that it is not the total open solar flux that has drifted; rather it is the latitudinal distribution of a constant open flux that has changed, such that heliospheric field has been increasingly concentrated at low latitudes.

[43] Analysis of both the first and the second perihelion pass of Ulysses (for which uncertainties caused by the r^2 correction and the propagation lag are minimized) shows that the uncertainty in the open flux derived from near-Earth measurements is less than 5% [*Lockwood et al.*, 2003]. As these two passes were close to solar minimum and maximum, we can say that the near-Earth methods are valid, at least over the last solar cycle, as also found for the rest of the Ulysses orbit by *Smith et al.* [2001]. The good agreement between $[F_S]_{IMF}$ and $[F_S]_{PFSS}$ for 1967–2001 reported by *Wang and Sheeley* [2002] and the good agreement between $[F_S]_{aa}$ and $[F_S]_{PFSS}$ reported here shows that the Ulysses result has also held throughout this interval.

[44] We have shown that all long-term data series on cosmic rays give very strong and highly significant anti-correlations with the near-Earth heliospheric field, as also reported by *Cane et al.* [1999] and *Lockwood* [2001]; even the well-known alternate rounded and peaked maxima in these fluxes is reflected in the open flux variations. This is significant because cosmic rays are shielded by the whole heliosphere and the exceptional agreement between the two (on timescales up to 50 years and thus revealing long-term drifts aa well as the solar cycles) implies that the drifts are not caused by a field increase that is restricted to low solar latitudes, with a matching decrease in the high-latitude heliospheric field. It has been predicted theoretically that drifts of cosmic rays may be important at sunspot minimum, and these depend on the polarity of the heliospheric field [*Jokipii*, 1991]. At sunspot minima at the start of even-numbered solar cycles (e.g., 1986), when the northern polar field is toward the Sun, cosmic rays are predicted to enter

the inner heliosphere preferentially along the heliospheric current sheet. (At sunspot maximum this drift effect is thought to be negligible compared with the effect of the diffusive barrier presented to cosmic ray by coronal mass ejections and other irregularities which merge together in the Parker spiral toward the termination shock). This could, arguably, be consistent with the contention by *Arge et al.* [2002] that the long-term drifts in the near-Earth heliospheric field are caused by the open flux accumulating near the heliospheric current sheet. However, at sunspot minima at the start of odd-numbered solar cycles (e.g., 1975), when the northern polar field is away from the Sun, cosmic rays would enter preferentially over the heliopsheric poles. The fact that both even and odd numbered cycles show the same long-term variations in cosmic ray fluxes is inconsistent with the latitudinal restructuring of the heliosphere proposed by Arge et al.

[45] The cosmic ray data, although giving an excellent anticorrelation with the open solar flux estimates from aa, do not in general extend back far enough to confirm the major long-term drift seen in $[F_S]_{aa}$ during solar cycles 14–19 (1900–1960). However, the early data from ionization chambers [*Neher et al.*, 1953; *Forbush*, 1958] are fully consistent with the open flux deduced from aa and do show a fall in the cosmic ray fluxes consistent with the observed rise in $[F_S]_{aa}$. *McCracken and McDonald* [2001] have noted the consistency of these early data with the ^{10}Be abundance record and discussed the implications for our understanding of how the Earth is shielded from cosmic rays.

[46] On yet longer timescales, the variation of $[F_S]_{aa}$ is highly consistent with the production of cosmogenic isotopes ^{10}Be and ^{14}C, found and dated from ice sheets and tree rings. It also matches very well the predictions of the simple model of open flux evolution by *Solanki et al.* [2000, 2002].

[47] **Acknowledgments.** The author is grateful for discussions with, and preprints from, a number of scientists concerning their recent work, in particular, S. Solanki, Y.-M. Wang, J. Kirkby, K. McCracken, T.D.G. Clark, and D.H. MacKay. He is also grateful to J. Beer, who supplied the ^{10}Be isotope data from the Dye3 Greenland ice core, to Y.-M. Wang who supplied the open flux values derived using the PFSS method, to A. Balogh and the team at Imperial College, London who supplied the Ulysses magnetometer data, to D. McComas who supplied the Ulysses solar wind data and to the World Data Center system for collecting, archiving, and distributing the cosmic ray data. This work was supported by the U.K. Particle Physics and Astronomy Research Council.

[48] Shadia Rifai Habbal thanks Yi-Ming Wang and another referee for their assistance in evaluating this paper.

References

Ahluwalia, H. S., Galactic cosmic ray intensity variations at a high-latitude sea-level site 1937–1994, *J. Geophys. Res.*, *102*, 24,229–24,236, 1997.

Arge, C. N., E. Hildner, V. J. Pizzo, and J. W. Harvey, Two solar cycles of nonincreasing magnetic flux, *J. Geophys. Res.*, *107*(A10), 1319, doi:10.1029/2001JA000503, 2002.

Balogh, A., E. J. Smith, B. T. Tsurutani, D. J. Southwood, R. J. Forsyth, and T. S. Horbury, The heliospheric field over the south polar region of the Sun, *Science*, *268*, 1007–1010, 1995.

Bard, E., G. M. Raisbeck, F. Yiou, and J. Jouzel, Solar modulation of cosmogenic nuclide production over the last millenium: Comparison between ^{14}C and ^{10}Be records, *Earth Planet. Sci. Lett.*, *150*, 453–462, 1997.

Beer, J., Long-term indirect indices of solar variability, *Space Sci. Rev.*, *94*, 53–66, 2000.

Beer, J., et al., Use of ^{10}Be in polar ice to trace the 11-year cycle of solar activity, *Nature*, *347*, 164–166, 1990.

Beer, J., S. Tobias, and N. Weiss, An active Sun throughout the Maunder minimum, *Sol. Phys.*, *181*, 237–249, 1998.

Bonino, G., G. Cini Castognoli, N. Bhabdari, and C. Taricco, Behavior of the heliosphere over prolonged solar quiet periods by ^{44}Ti measurements in meteorites, *Science*, *270*, 1648–1650, 1998.

Cane, H. V., G. Wibberenz, I. G. Richardson, and T. T. von Rosenvinge, Cosmic ray modulation and the solar magnetic field, *Geophys. Res. Lett.*, *26*, 565–568, 1999.

Clilverd, M. A., T. D. G. Clark, E. Clarke, and H. Rishbeth, Increased magnetic storm activity from 1868 to 1995, *J. Atmos. Sol.-Terr. Phys.*, *60*, 1047–1056, 1998.

Cliver, E. W., V. Boriakoff, and K. H. Bounar, The 22-year cycle of geomagnetic activity, *J. Geophys. Res.*, *101*, 27,091–27,109, 1996.

Couzens, D. A., and J. H. King, *Interplanetary Medium Data Book*, suppl. 3, Natl. Space Sci. Data Cent., Goddard Space Flight Cent., Greenbelt, Md., 1986.

Forbush, S. E., Cosmic ray intensity variations during two solar cycles, *Geophys. Res.*, *63*, 651–669, 1958.

Foster, S., and M. Lockwood, Long-term changes in the solar photosphere associated with changes in the coronal source flux, *Geophys. Res. Lett.*, *28*, 1443–1446, 2001.

Gazis, P. R., Solar cycle variation of the heliosphere, *Rev. Geophys.*, *34*, 379–402, 1996.

Gleissberg, W., A table of secular variations of the solar cycle, *J. Geophys. Res.*, *49*, 243–244, 1944.

Hapgood, M. A., A double solar-cycle variation in the 27-day recurrence of geomagnetic activity, *Ann. Geophys.*, *11*, 248–256, 1993.

Harvey, K. L., and C. Zwaan, Properties and emergence of bipolar active regions, *Sol. Phys.*, *148*, 85–118, 1993.

Jokipii, J. R., Variations of the cosmic ray flux with time, in *The Sun in Time*, edited by C. P. Sonnet, M. S. Giampapa, and M. S. Matthews, pp. 205–221, Univ. of Ariz. Press, Tucson, Ariz., 1991.

Lockwood, M., Long-term variations in the magnetic fields of the Sun and the heliosphere: Their origin, effects, and implications, *J. Geophys. Res.*, *106*, 16,021–16,038, 2001.

Lockwood, M., An evaluation of the correlation between open solar flux and total solar irradiance, *Astron. Astrophys.*, *382*, 678–687, 2002a.

Lockwood, M., The relationship between the near-Earth interplanetary field and the coronal source flux: Dependence on timescale, *J. Geophys. Res.*, *107*(A12), 1425, doi:10.1029/2001JA009062, 2002b.

Lockwood, M., and R. Stamper, Long-term drift of the coronal source magnetic flux and the total solar irradiance, *Geophys. Res. Lett.*, *26*, 2461–2464, 1999.

Lockwood, M., R. Stamper, and M. N. Wild, A doubling of the Sun's coronal magnetic field during the last 100 years, *Nature*, *399*, 437–439, 1999a.

Lockwood, M., R. Stamper, M. N. Wild, A. Balogh, and G. Jones, Our changing Sun, *Astron. Geophys.*, *40*, 4.10–4.16, 1999b.

Lockwood, M., R. B. Forsyth, A. Balogh, and D. J. McComas, The accuracy of open solar flux estimates from near-Earth measurements of the interplanetary magnetic field: Analysis of the first two perihelion passes of the Ulysses spacecraft, *Ann. Geophys.*, in press, 2003.

Mackay, D. H., E. R. Priest, and M. Lockwood, The evolution of the Sun's open magnetic flux, I, A single bipole, *Solar Phys.*, *207*(2), 291–308, 2002a.

Mackay, D. H., E. R. Priest, and M. Lockwood, The evolution of the Sun's open magnetic flux, II, Full solar cycle simulations, *Solar Phys.*, *209*(2), 287–309, 2002b.

Mayaud, P. N., The *aa* indices: A 100-year series characterizing the magnetic activity, *J. Geophys. Res.*, *77*, 6870–6874, 1972.

McCracken, K. G., and F. B. McDonald, The long-term modulation of the galactic cosmic radiation, 1500–2000, in *Proceedings of the 27th International Cosmic Ray Conference, Hamburg*, in press, 2001.

Neher, H. V., V. Z. Peterson, and E. A. Stern, Fluctuations and latitude effect of cosmic rays at high altitudes and latitudes, *Phys. Rev.*, *90*, 655–674, 1953.

Nevanlinna, H., and E. Kataja, An extension to the geomagnetic activity index series aa for two solar cycles (1844–1868), *Geophys. Res. Lett.*, *20*, 2703–2706, 1993.

O'Brien, K., Secular variations in the production of cosmogenic isotopes in the Earth's atmosphere, *J. Geophys. Res.*, *84*, 423–431, 1979.

Pulkkinen, T. I., H. Nevanlinna, P. J. Pulkkinen, and M. Lockwood, The Earth-Sun connection in time scales from years to decades to centuries, *Space Sci. Rev.*, *95*, 625–637, 2001.

Schatten, K. H., Models for coronal and interplanetary magnetic fields: A critical commentary, in *Sun-Earth Plasma Connections*, *Geophys. Monogr. Ser.*, vol. 109, edited by J. L. Burch, R. L. Carovillano, and S. K. Antiochos, pp. 129–142, AGU, Washington, D.C., 1999.

Smith, E. J., A. Balogh, R. J. Forsyth, and D. J. McComas, Ulysses in the south polar cap at solar maximum: Heliospheric magnetic, *Geophys. Res. Lett.*, *28*, 4159–4162, 2001.

Solanki, S. K., M. Schüssler, and M. Fligge, Secular evolution of the Sun's magnetic field since the Maunder minimum, *Nature*, *480*, 445–446, 2000.

Solanki, S. K., M. Schüssler, and M. Fligge, Secular variation of the Sun's magnetic flux, *Astron. Astrophys.*, *383*, 706–712, 2002.

Stamper, R., M. Lockwood, M. N. Wild, and T. D. G. Clark, Solar causes of the long term increase in geomagnetic activity, *J. Geophys Res.*, *104*, 28,325–28,342, 1999.

Stuiver, M., and P. D. Quay, Changes in atmospheric carbon-14 attributed to a variable Sun, *Science*, *207*, 11, 1980.

Suess, S. T., and E. J. Smith, Latitudinal dependence of the radial IMF component—Coronal imprint, *Geophys. Res. Lett.*, *23*, 3267–3270, 1996.

Suess, S. T., E. J. Smith, J. Phillips, B. E. Goldstein, and S. Nerney, Latitudinal dependence of the radial IMF component—Interplanetary imprint, *Astron. Astrophys.*, *316*, 304–312, 1996.

Ulrich, R. K., Analysis of magnetic flux tubes on the solar surface from observations at Mt. Wilson of λ5250 and λ5233, in *Cool Stars, Stellar Systems and the Sun*, edited by M. S. Giampapa and J. A. Bookbinder, p. 265, Astron. Soc. of the Pacific, San Francisco, Calif., 1992.

Vasyliunas, V. M., J. R. Kan, G. L. Siscoe, and S.-I. Akasofu, Scaling relations governing magnetospheric energy transfer, *Planet Space Sci.*, *30*, 359–365, 1982.

Wang, Y.-M., and N. R. Sheeley Jr., Solar implications of Ulysses interplanetary field measurements, *Astrophys. J.*, *447*, L143–L146, 1995.

Wang, Y. M., and N. R. Sheeley Jr., Sunspot activity and the long-term variation of the Sun's open magnetic flux, *J. Geophys. Res.*, *107*(A10), 1302, doi:10.1029/2001JA000500, 2002.

Wang, Y.-M., N. R. Sheeley Jr., and J. Lean, Understanding the evolution of Sun's magnetic flux, *Geophys. Res. Lett.*, *27*, 621–624, 2000a.

Wang, Y.-M., J. Lean, and N. R. Sheeley Jr., The long-term evolution of the Sun's open magnetic flux, *Geophys. Res. Lett.*, *27*, 505–508, 2000b.

Wilks, D. S., *Statistical Methods in the Atmospheric Sciences*, Academic, San Diego, Calif., 1995.

M. Lockwood, Space Science and Technology Department, Rutherford Appleton Laboratory, Chilton, Didcot, Oxfordshire, OX 11 0QX, UK. (m.lockwood@rl.ac.uk)